Escape time of heliumlike α resonance-line photons emitted from optically thick plasmas

J. P. Apruzese
Radiation Hydrodynamics Branch, Plasma Physics Division, Naval Research Laboratory, Washington, D.C. 20375
(Received 12 November 1992)

The heliumlike α resonance line is one of the strongest and most frequently observed transitions in plasma spectroscopy. In optically thick plasmas of moderate density, photons emitted in this line typically undergo many absorptions and reemissions before escaping. In the present investigation the time required for this process to occur in aluminum plasma is calculated by numerical solution of the time-dependent equation of radiative transfer, in which the photon transit time between interactions is taken into account. An analytic model is also developed in which the collisional quenching probability is parametrized in terms of an equivalent two-level atom. This model facilitates interpretation of the numerical results and permits economical estimates of the escape time for different plasma elements and conditions. One practical implication of these results is that a subpicosecond x-ray pulse from a femtosecond laser-produced high-density plasma can be broadened by multiple scattering if it propagates into a moderate-density preformed plasma.

PACS number(s): 52.25.Nr, 32.30.Rj, 52.65.+z, 41.50.+h

I. INTRODUCTION

The $1s^2-1s2p\ ^1P_1$ principal resonance line of the heliumlike ion (designated He-α) is one of the most frequently observed lines in plasma spectroscopy. It has been detected in devices ranging from tokamaks to inertial confinement fusion capsules to Z pinches. Most recently, this line has appeared prominently in the spectra of targets irradiated by high-power sub-ps lasers.

For elements with atomic number Z between 4 and 50, the oscillator strength of this transition [1] exceeds 0.5, hence it is usually optically thick for moderate- to high-density plasmas. The associated rapid spontaneous decay rate means that absorption of a line photon is often followed by reemission within the line profile (referred to as scattering). Thus, much of the line energy that escapes the plasma does so after diffusion in both position and frequency, which can affect the intensity and width of the x-ray pulse. For multi-ns sources such as the dense Z pinch, this effect is expected to be small compared to the inherent lifetime of the plasma. However, this may not be the case for the very-short-lived plasmas produced by the current generation of powerful sub-ps lasers [2–12]. Numerous uses of such plasmas are envisioned, prominently among them the production of ultrashort x-ray pulses [2,4,5,12–16].

One interesting phenomenon which has been identified and quantified to some degree is the effect of a laser prepulse on the characteristics of the x rays emitted from such short-lived plasmas. Cobble and co-workers [7,17] and others [10] report that the presence of a prepulse has a strongly positive effect on the plasma x-ray yield. This occurs whether the prepulse is of nsec [7,17] or sub-ps [10] duration. With a prepulse present, the preformed plasma may have time to expand, and, as pointed out in Refs. [14–16], expansion and thermal conduction are potentially important cooling mechanisms in these plasmas. The greater the scale length, the more these mechanisms tend to broaden the x-ray pulse. A tradeoff between yield and pulsewidth thus appears to be indicated.

It is the relatively large preformed plasmas producing the best x-ray yields which are also the most likely to be affected by pulse broadening inherent in the multiple scattering of strong x-ray lines. The purpose of the present work is to quantify the escape time of the He-α-line radiation. Section II presents the numerical and analytic models of radiation transport used in the calculation. The numerical calculations are done for aluminum, which has been a frequent experimental target for sub-ps lasers [5,7,10,17], and from which the He-α line has been strongly detected. In Sec. III, the validity of the analytic model is assessed by direct comparison with numerical results. The analytic model is extendable to elements other than aluminum. Results for different plasma conditions are also presented and discussed.

II. RADIATION TRANSPORT

A. Numerical model

The time-dependent transport of radiation of frequency ν along a ray in the positive-x direction is described by the equation of transfer

$$\frac{\partial I_\nu}{\partial x}=j_\nu-k_\nu I_\nu-\frac{1}{c}\frac{\partial I_\nu}{\partial t}\ . \tag{1}$$

In Eq. (1), I_ν is the specific intensity, j_ν and k_ν are the emission and absorption coefficients, and c is the velocity of light. For a derivation of this equation see, e.g., Ref. [18]. Consider the space-time point (x_0,t_0). Looking in the negative-x direction, the quantities determining $I_\nu(x_0,t_0)$ are j_ν and k_ν encountered at retarded times $t_r(x_0,t_0,x)=t_0-[(x_0-x)/c]$. The effective optical depth between x_0 and x at time t_0 is

$$\tau_\nu(x_0,t_0,x)=\int_x^{x_0} k_\nu(t_r)dx \ , \tag{2}$$

and the solution to Eq. (1) is

$$I_\nu(x_0,t_0)=\int_{x_b}^{x_0} j_\nu(x,t_r(x)) \times \exp[-\tau_\nu(x_0,t_0,x)]dx \ . \tag{3}$$

In Eq. (3), x_b is the coordinate of the plasma boundary. In all cases to be considered, it is assumed that no external x rays are incident on the plasma. Given the emission and absorption coefficients from previous time steps, Eq. (3) is numerically solved on a grid of 31 frequency points within the line profile and a spatial mesh of 26–31 points per ray. Linear interpolation in both space and time is employed for j_ν and k_ν. The maximum time step employed is 10 fs. To compute photoexcitation and escape rates, the angle-averaged intensity J_ν and net radiative flux F_ν are needed. This requires an assumption for the shape and dimensionality of the medium. The present work will be confined to one-dimensional plane-parallel geometry. The numerical burden of including full time dependence in the radiative transfer is kept at an acceptable level with this simple choice of geometry. Also, the optical depth presented to an escaping line photon can be unambiguously characterized and associated with a calculated escape time or probability. This will facilitate analysis of future multidimensional work more representative of actual laboratory plasmas.

The distribution of the rays follows Gaussian quadrature as described by Chandrasekhar in Ref. [19]. Each ray is characterized by the cosine of its angle ($\mu=\cos\theta$) to the planar normal. In the present work both four rays and two rays have been employed for comparison. Their specific μ's are given in Table III of Ref. [19]. In planar, one-dimensional geometry the quantities J_ν and F_ν are given by

$$J_\nu=\tfrac{1}{2}\int_{-1}^{+1} I_\nu(\mu)d\mu \ , \tag{4}$$

$$F_\nu=2\pi\int_{-1}^{+1} I_\nu(\mu)\mu\, d\mu \ . \tag{5}$$

The line photon escape rate is the frequency integral of F_ν at the plasma boundary. The photoexcitation rate for a spectral line of absorption oscillator strength f_{lu} from lower level l to upper level u is given by

$$W_{lu}(\sec^{-1})=\frac{\pi e^2}{mc} f_{lu}\int \frac{4\pi J_\nu}{h\nu}\phi_\nu d\nu \ , \tag{6}$$

where the integral is taken over the line profile ϕ, whose normalization is $\int\phi_\nu d\nu=1$. Given the photoexcitation rates as well as the appropriate set of collisional rates, populations of the various levels and ionic stages are obtained as a function of time by numerical integration of the atomic rate equations (see, e.g., Eq. (1) of Ref. [20]). The method of Young and Boris [21] is employed, as it is especially well suited to the time integration of numerically stiff differential equations.

B. Analytic model

The two-level-atom approximation has been treated extensively in the astrophysical literature (see, e.g., Ref. [22] and references cited therein). It is therefore a natural starting point for an analytic description of the radiative transfer within the He-α line. Even though the heliumlike ion is obviously not a two-level system, the same processes of scattering and collisional quenching are operative in determining the fate of the emitted line photons. Upon absorption, the photon will either be reemitted or various other processes will transfer the $1s2p\ ^1P_1$ electron elsewhere. For the idealized two-level-atom case, "elsewhere" is only the ground state. For the real heliumlike ion, the electron can in principle end up almost anywhere within the same ion or the adjoining hydrogenic or lithiumlike species. One cannot obtain a probability of collisional quenching (designed ϵ) by merely adding the rates to all other possible levels from $1s2p\ ^1P_1$, since in some cases the electron is collisionally shunted right back to the original upper level of the transition. It is necessary to subtract (for each transition) the probability that the electron returns to the $1s2p\ ^1P_1$ level.

If the electron is transferred to level i from the $1s2p\ ^1P_1$ state, the probability of return to the $1s2p\ ^1P_1$ level P_{ri} is defined as the rate from level i back to $1s2p\ ^1P_1$ divided by the sum of all the rates out of level i. The net quenching probability ϵ is then given by

$$\epsilon=\frac{\sum_i C_i(1-P_{ri})}{A_{ul}+\sum_i C_i(1-P_{ri})} \ . \tag{7}$$

In Eq. (7), C_i is the rate from $1s2p\ ^1P_1$ to the ith level, A_{ul} is the spontaneous decay rate of the resonance transition, and the sum is taken over all levels connected to $1s2p\ ^1P_1$.

The quenching probability ϵ has been computed for Al using the atomic data described in Ref. [20]. From the $1s2s\ ^1S_0$ level the chance of return to the $1s2p\ ^1P_1$ level is appreciable (0.92 at an electron density of 10^{21} cm^{-3} near temperatures of 200 eV). At these same conditions, the net probability of collisional quenching of the Al He-α line per absorption (ϵ) is 0.029.

Line photons may also be eliminated from the plasma by escape. The probability P_e that the photon escapes a medium of a given optical depth is obtained from a weighted average of the exponential escape probability at each frequency within the line profile. The weighting factor is the strength of the profile itself at each frequency. Detailed treatment of escape probability calculations may be found in Refs. [23–27]. For stationary media, useful analytic forms have been obtained for Doppler [23,24], Voigt [25], and Stark [26,27] line profiles. The Doppler shift due to bulk motion can influence P_e in some instances. For media where this is important, the original work of Sobolev [28] has recently been extended by Shestakov and Eder [29] to include cylindrical geometry.

The quantities ϵ and P_e discussed above, along with the spontaneous decay rate of the upper level A_{ul}, suffice for an appropriate analytic description of line photon escape

and transport. The probability that a photon escapes after an excitation is $(1-\epsilon)P_e$, whereas the probability that it remains within the plasma is $S \equiv (1-\epsilon)(1-P_e)$. The probability that the photon has escaped by the Nth scattering is the sum of the probabilities of escape after initial excitation and each of the subsequent scatterings, viz.

$$P_N = (1-\epsilon)P_e \left[1 + \sum_{n=1}^{N} S^n \right] = (1-\epsilon)P_e \left[\frac{1-S^N}{1-S} \right] . \quad (8)$$

The ultimate escape probability is obtained by taking the limit of Eq. (8) as $N \rightarrow \infty$, $P_u = P_e(1-\epsilon/1-S)$. The time required for N scatterings, i.e., the time associated with line photon probability of escape P_N, including the initial excitation but ignoring the photon travel time between absorptions, is simply the level lifetime A_{ul}^{-1} multiplied by $N+1$. Thus, P_N given by Eq. (8) is equivalently $P(t)$, where $t = (N+1)/A_{ul}$. This analytic form for the fraction of line photons which have escaped as a function of time is compared in the next section with numerical results. It is straightforward to obtain an explicit expression for the time for fractional escape f_e (of the photons which ultimately escape). The condition is $f_e = 1-S^N$, which leads to

$$t(f_e) = A_{ul}^{-1} \left[\frac{\ln(1-f_e)}{\ln S} + 1 \right] , \quad (9)$$

and in the limit $P_e, \epsilon \ll 1$,

$$t(f_e) = A_{ul}^{-1} \left[\frac{\ln(1-f_e)}{-(P_e+\epsilon)} + 1 \right] . \quad (10)$$

It is possible to construct an analytical model using three or more levels. However, as pointed out in Ref. [30], the algebra quickly becomes unmanageable. Moreover, as seen below, the equivalent two-level approach yields respectable accuracy as well as considerable physical insight. Note also that a single P_e is employed despite the fact that in principle it varies between subsequent scatterings when the photon is emitted from a different position in the plasma. However, as has been shown previously [31,32], the line photon usually remains imprisoned within the line core and stays close to its location of previous emission, escaping in one long flight when emitted in the line wing. Although somewhat oversimplified, this picture explains the success of this approximation in both the present and previous work. As is evident in the next section, some spatial diffusion of the excitation does occur.

III. RESULTS

A. Equivalent two-level atom

The calculations presented in this section have two principal objectives: first, to assess whether under the chosen conditions transport of the principal resonance line of the heliumlike ion can be understood and parametrized as if the ion consisted merely of a ground and one excited state; second, to establish the numerical parameters needed to insure accuracy in the computation. As stated above in Sec. II B, at an electron density of 10^{21} cm^{-3}, and temperatures around 200 eV the net probability of collisional quenching per absorption for the Al He-α line is 0.029. A two-level-atom test case is chosen to correspond to this value. At this density, the line is well described by a Voigt profile whose broadening parameter $a = 0.05$. A planar Al plasma of width 100 μm would have about 90% of its ions in the heliumlike stage under these conditions. The line center optical depth τ_0 of the He-α line, measured normally from the midplane to plasma boundary, is 90. These are the conditions for which the present calculations were run; obviously, no extensive atomic data file is required for this simplified case. The plasma is assumed stationary (i.e., bulk Doppler motion is neglected in the radiative transfer). To examine the diffusion and escape of line photons, the following initial excitation conditions are assumed: the ions are entirely in the ground state except for the spatially innermost 12%, where 1% of the ions are in the excited state; see Fig. 1. The clock starts at $t = 0$ and the line photons begin escaping and migrating toward the plasma boundary. The collisional excitation rate is set to zero as if the plasma cools instantaneously. In this fashion, the spatial diffusion and escape times obtained reflect only the effects of radiative transfer.

The upper-level fraction as a function of space and time is illustrated in Figs. 1 and 2 for 5 time points varying from 0 to 7 psec, for both four-ray and two-ray Gaussian quadrature. Note first the excellent agreement between the $n = 2$ and 4 cases, strongly suggesting that two rays are adequate. Spatial diffusion of the upper-level population due to line photon absorption and reemission is clearly evident. Of considerable interest is the rate of decay of the upper-level population in the central

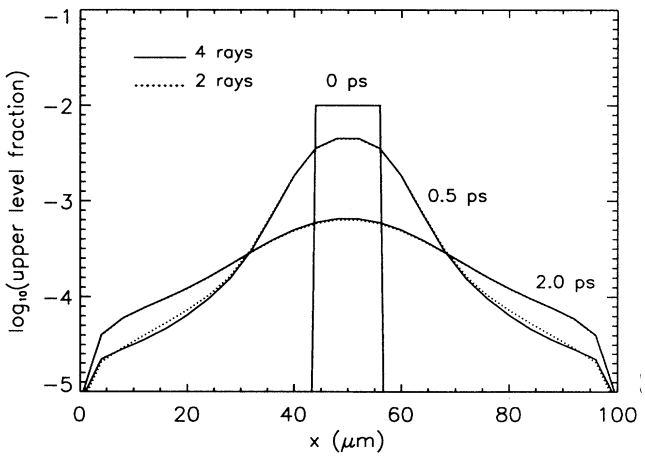

FIG. 1. Al XII $1s2p\ ^1P_1$ population fraction is shown as a function of space and time in the two-level-atom approximation at 0, 0.5, and 2.0 ps following initial excitation. The plasma is planar, 100 μm thick, with an assumed temperature of 200 eV and electron density 10^{21} cm^{-3}. Differing assumptions of the various calculations are as indicated in the figure and discussed in the text.

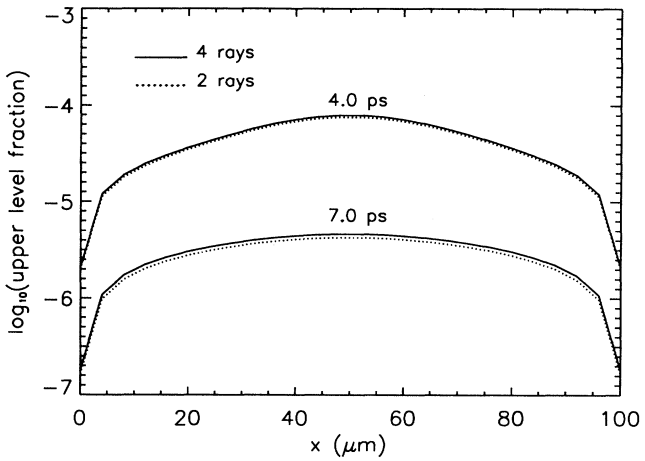

FIG. 2. As in Fig. 1, except that times of 4.0 and 7.0 ps after initial excitation are illustrated.

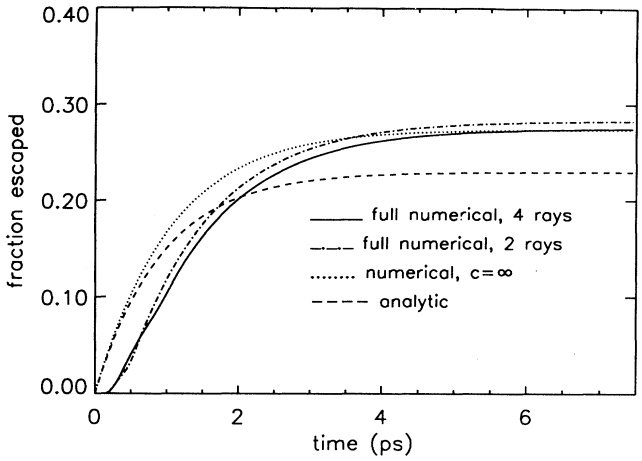

FIG. 3. Escaped photon fraction for the Al He-α line is illustrated for the conditions of Figs. 1 and 2 as a function of time. Numerical calculations using four Gaussian rays assuming both the correct and infinite light velocity are shown, as well as two-ray and analytic approximations discussed in the text.

zone. If the plasma were optically thin, this population would decrease with an e-folding time of $A_{ul}^{-1}=36$ fsec. The actual lifetime is much greater in the optically thick medium because of reexcitation of the level by the line photons, as is evident in Figs. 1 and 2. For the first 0.5 psec, the effective lifetime of the upper level is 0.7 psec, increasing to 1.1 psec for the final 3 psec covered by Figs. 1 and 2. A frequently used approximation for line transfer is to multiply the spontaneous decay rate by the escape probability, to obtain an effective decay rate which compensates for reabsorption. The results of Ref. [25] may be used to obtain a planar average escape probability P_e of 8.9×10^{-3} for this case. Including the effects of collisional depletion of the upper level, the total effective decay rate is $\sim A_{ul}(P_e+\epsilon)=1.05\times10^{12}$ sec^{-1}, implying a lifetime of 0.95 psec. This value is very close to the average e-fold time observed in Figs. 1 and 2. Transient delays in reexcitation result in an initially more rapid population falloff, but this phenomenon damps out over 7 ps, resulting in good correspondence between the analytically estimated and numerically computed upper-level decay times.

The time profile of escape of the He-α line photons is illustrated in Fig. 3, where numerical results are plotted along with the analytic solution of Eqs. (8) and (9). As indicated in that figure, one of the numerical calculations ignored the time-dependent term in Eq. (1), therefore implicitly neglecting the photon travel time. The analytic solution also neglects this effect. The numerical solutions which do include full time dependence were obtained for both two and four Gaussian rays, and, as evident in Fig. 3, the agreement is excellent. All results presented in succeeding sections were therefore obtained using the more economical two-ray approximation.

The asymptotic or ultimate escape probability $P_u=P_e(1-\epsilon/1-S)$ is 0.23 for the escape and quenching probabilities quoted above. Most of the emitted He-α photons do not escape, since the quenching probability ($\epsilon=0.029$) exceeds that of escape ($P_e=8.9\times10^{-3}$) by a factor of 3. The fully-time-dependent numerical solutions depart from the analytic result in several details. First, the photons do not emerge immediately since 170 fsec is required to traverse the 50 μm from the center to the outer boundary of the plasma. Also, about 28% of the initially created line photons escape rather than the 23% given by the analytic solution. This is not particularly surprising, since the fixed escape probability is computed from the plasma midplane but the photons diffuse spatially toward the boundary and therefore should not strictly obey a single escape probability. According to the fully-time-dependent numerical calculation, 1.3 psec is required for 50% of the photons to escape. Achieving a sub-psec x-ray pulse in Al He-α may be difficult for a plasma like the present one, where the line scatters many times prior to escape. Note that recombination of the heliumlike species occurs on a time scale of ≥ 10 psec [5], even for electron densities of $\sim10^{22}$ cm^{-3}. Therefore, it will not eliminate the source of the multiple scattering during the x-ray pulse. For near solid density plasmas, three-body recombination is fast enough to short circuit this mechanism. More general conditions and assumptions are now examined, and more favorable plasma properties conducive to shorter pulses are considered.

B. Multilevel aluminum plasma

In this section, the simplifying approximation of a parametrized two-level atom is dropped and the escape and diffusion of the He-α line is examined with a multistage, multilevel atomic model for aluminum ions. Due to the expense of such fully-time-dependent calculations, it was not feasible to do a truly comprehensive set of runs closely covering all of the expected conditions where such effects might be important. Nevertheless, with the aid of the analytic model discussed above and the atomic num-

ber scaling considerations presented below, essential conclusions can be drawn for much of the important physics as applied to frequently achieved conditions in laboratory experiments.

The aluminum atomic model emphasizes the heliumlike stage where excited levels are carried ranging through $n=7$. Triplet and singlet sublevels are modeled for $n=2$ and 3, but $n=4-7$ are treated as Rydberg levels in which the triplets and singlets are assumed to be populated statistically. A total of 33 ground and excited states are included in the neutral through bare nuclear stages. The heliumlike rates affecting the $n=2$ sublevels are of the most importance for the present study and are in good agreement with those of Zhang and Sampson [33]. For the methods used for the atomic rate calculations, the reader may consult Ref. [20] and references cited therein.

The profile of the Al He-α line is assumed to be described by the Voigt function with the broadening parameter obtained by summing the rates out of the upper and lower levels. This line is one of the last transitions in the heliumlike manifold to be affected by Stark broadening as density increases. Detailed calculations of the Stark profile of He-α have been presented in Ref. [34], for neon and argon, for typical temperatures at which these ions exist. For neon ($Z=10$), the Stark profile is less than 10% of the Doppler width for electron densities $\leq 10^{22}$ cm^{-3}. In the case of argon ($Z=18$), electron density of at least 2×10^{23} is needed for the Stark width to exceed 10% of the Doppler width. According to Ref. [35], the Stark width in eV scales as $N_e^{2/3}Z^{-1}$. The temperature at which the heliumlike stage exists is approximately proportional to Z^3 [33], the ionic mass scales as Z, and line energy as Z^2, leading to a line Doppler width scaling of Z^3. Therefore, the electron density at which the line Stark-to-Doppler width ratio is a constant 0.1 would scale as Z^6. The detailed calculations quoted above are in reasonable accord with this approximation at $Z^{5.1}$. It is concluded that for aluminum, the Stark width of the He-α line would not exceed 10% of the Doppler width except for electron densities $\geq 4\times10^{22}$ cm^{-3}. At such densities, the collisional quenching parameter exceeds 0.5, and the line photons can no longer undergo multiple scattering. Therefore, for present purposes, the Voigt profile approximation is reasonable.

Results of the detailed configuration multilevel calculations for aluminum are shown in Figs. 4–7. In Figs. 4–6, the total ion density is assumed to be 3.0×10^{19}, 9.1×10^{19}, and 9.1×10^{20} cm^{-3}, respectively. A calculation at solid density (6×10^{22} cm^{-3}) was also done and is discussed below. The plasma thickness is 100 μm in Figs. 4 and 5, but 10 μm in Fig. 6. In each case the plasma temperature is 200 eV, but there is no reason to expect qualitative differences for any temperature at which the heliumlike stage dominates (i.e., 150–400 eV for Al). As is evident from the "$t=0$" curves in these figures, the initial conditions are essentially the same as for the two-level-atom case. Initially, the innermost 10% of the planar plasma has the $1s2p\ ^1P_1$ level excited to a fractional population of 0.01. The spread of excitation due to the diffusion of the He-α line photons is apparent.

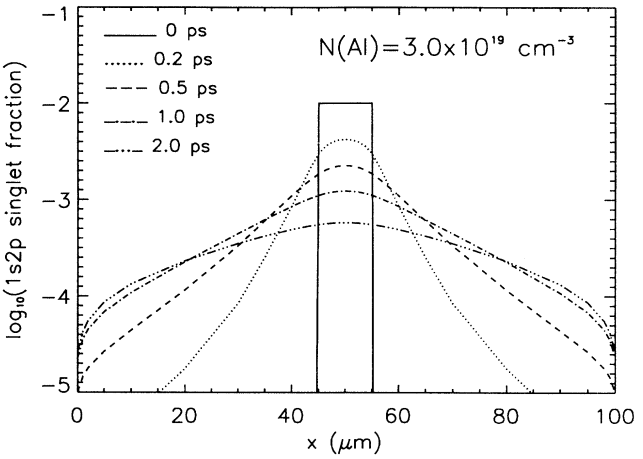

FIG. 4. Al XII $1s2p\ ^1P_1$ population fraction is shown as a function of space and time as obtained from a multilevel fully-time-dependent coupled rate and radiative transfer calculation as described in the text. The planar, 100-μm-thick plasma has an assumed temperature of 200 eV and total ion density of 3.0×10^{19} cm^{-3}.

Modification of the escape probability due to the Doppler shift of plasma bulk motion was not taken into account; such effects are discussed in the next section.

As the electron density increases in Figs. 4–6, the collisional quenching probability per scattering ϵ increases from 0.01 (Fig. 4) to 0.029 (Fig. 5) to 0.23 (Fig. 6). The single flight photon escape probabilities P_e for these three cases are 1.6×10^{-2}, 8.9×10^{-3}, and 1.5×10^{-2}, respectively. Even though the column density of plasma represented in Figs. 5 and 6 is the same, the escape probability increases at the higher density due to the enhancement of the optically thin line wings in the assumed Voigt profile. However, the ultimate escape probability P_u that a photon leaves the plasma after one or multiple scatterings, drops monotonically with increasing density be-

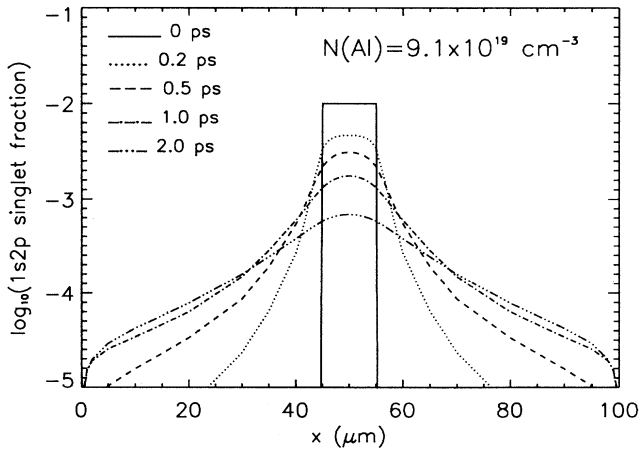

FIG. 5. As in Fig. 4, except that the total ion density is 9.1×10^{19} cm^{-3}, yielding an electron density of 10^{21} cm^{-3}.

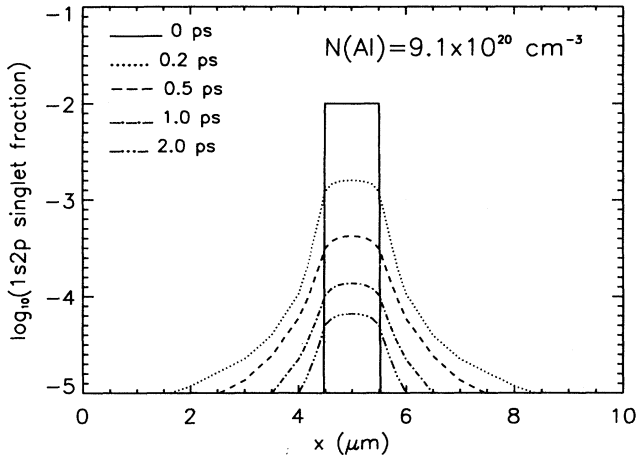

FIG. 6. As in Figs. 4 and 5, except that the total ion density is 9.1×10^{20} cm^{-3}, and the plasma thickness is 10 μm.

cause of the dominant influence of collisional quenching. The expression given in Sec. II B yields $P_u=0.61$, 0.23, and 0.05 for the conditions of Figs. 4–6, respectively. The differing collisional destruction of the He-α photons is clearly evident in Figs. 4–6. The spatial spread of excitation with time is much more pronounced in the lower-density cases of Figs. 4 and 5, whereas at the ion density of 9.1×10^{20} cm^{-3} represented by Fig. 6, it is very difficult for a typical He-α photon to run the gauntlet of collisional destruction and reach the plasma boundary. The conditions of Fig. 5 are nearly identical to those for which the parametrized two-level-atom case (Figs. 1–3) was studied in the preceding section. The excitation profiles as a function of time for the multilevel and two-level-atom cases may be compared in Figs. 1 and 5 at 0.5 and 2.0 ps. They show very good qualitative agreement; exact correspondence is not expected, since quenching of the line is affected by multilevel kinetics.

Figure 7 quantifies the time dependence of the escape

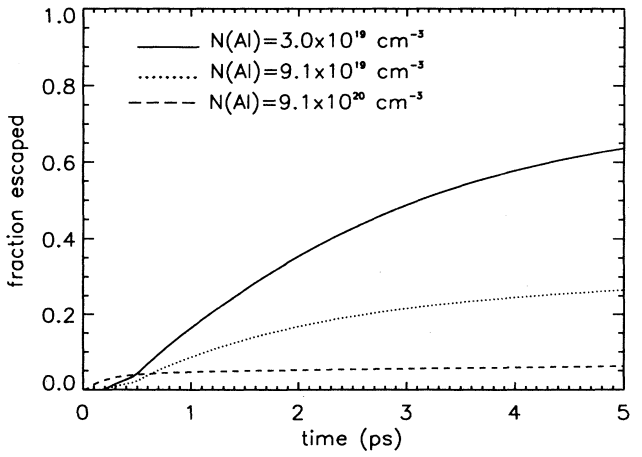

FIG. 7. Escaped photon fraction is plotted as a function of time for the Al He-α line. Total Al-ion densities and other plasma conditions are as assumed in Figs. 4–6.

of the He-α line radiation for these three cases as calculated with the detailed multilevel model. At $t=5$ ps, nearly all the photons have escaped and the values of each of the curves of Fig. 7 may be taken as a good estimate of P_u. They indicate that the analytic model predictions quoted above are quite respectable estimates: 0.61, 0.23, and 0.05 versus the computed values of 0.64, 0.27, and 0.07. Of course, the exact escape time is partly a matter of definition, but half the photons which ultimately will escape have escaped within ~0.3 ps for the highest density case, ~1.6 ps for the medium density of 9.1×10^{19} cm^{-3}, and within ~1.8 ps at the lowest density considered. At high density, the photons are quenched if they do not escape the plasma on first flight or after a few scatterings, hence the short pulsewidth. At the solid ion density of 6.0×10^{22} cm^{-3}, the quenching probability for Al is 0.95, and a detailed calculation confirmed the obvious expectation that the photon either escapes after initial collisional excitation of the $1s2p\ ^1P_1$ level, or is destroyed. No spatial diffusion occurs in this situation and no lower limit on the pulsewidth is set by these effects. The higher-level resonance lines of the heliumlike ion are of little significance for the present considerations. They are nearly always much weaker spectroscopically than the principal $n=2$ resonance line. Also, the higher lines are much more susceptible to collisional quenching because the radiative decay rates are lower and the collisional rates from the upper levels are much higher than those of He-α.

C. Generalized plasma conditions

1. *Effect of bulk motion*

It is well known that the frequency Doppler shift of the line profile due to expansion or compression of a medium can significantly enhance the escape probability. For planar geometry (to which the present work is confined), P_e may be calculated according to the method of Sobolev [28] when the velocity gradient is constant. Reference [29] extends Sobolev's work to cylindrical media. The frequent occurrence of regions of nearly constant velocity gradient in numerical and analytic solutions of plasma hydrodynamic behavior has fostered widespread use of these methods to obtain line escape probabilities. A full numerical treatment would require solution of the radiative transfer equation in the comoving frame. However, the analytic model embodied in Eqs (5) and (6) needs no modification, only the substitution of the Sobolev escape probability for the static one. The effect of motional Doppler shifts may already have been detected in the observed broadening of heliumlike Al lines [36].

The magnitude of the effect may be estimated using the analytic solution for isothermal plasma expansion discussed in Ref. [37]. The ion acoustic velocity for Al is $\sim10^7$ cm s^{-1} at 200 eV. A 1-ns prepulse would allow plasma expansion to ~100 μm, implying a velocity gradient of 10^9 s^{-1}. Two examples of 100-μm planar Al plasmas were discussed above in the static limit. For the low-density case of 3.0×10^{19} ions cm^{-3}, the motionally induced escape probability, calculated from Eq. (40) of

Ref. [28], is 8.0×10^{-3}, compared to 1.6×10^{-2} for the static limit. At the higher density of 9.1×10^{19} cm^{-3}, the Sobolev escape probability is 2.6×10^{-3}, as opposed to the static value of 8.9×10^{-3}. At this assumed velocity gradient, therefore, the escape probability is at most only slightly enhanced by motion and little effect is anticipated.

However, higher-velocity gradients than 10^9 s^{-1} are anticipated in some instances, especially for kV-temperature plasmas, as seen in the simulations of Ref. [36], where values of 2×10^{10} s^{-1} are calculated within 1 ps of the main pulse. Applying this much-higher-velocity gradient to the two plasmas discussed above increases P_e to 0.16 and 0.053, at densities of 3.0 and 9.1×10^{19} cm^{-3}, respectively. According to Eq. (10), the time for half of the He-α photons to escape would be reduced by factors of 5 and 2 for the two cases, respectively. It is therefore possible that motional broadening effects may significantly shorten the pulsewidth of a strong x-ray line, depending on the details of the particular plasma's hydrodynamics.

2. *Atomic number scaling*

The potential for broadening of the pulsewidth of a line is greatest when both the escape and quenching probabilities are small, allowing many scatterings within the plasma. In this limit, according to Eq. (10), the escape time scales as

$$t_e \sim [A_{ul}(P_e+\epsilon)]^{-1} . \tag{11}$$

Given current experimental capabilities, the atomic number region $8 \le Z \le 20$ is of most interest for production of significant K-shell emission. The spontaneous decay rate for He-α has been calculated and tabulated as a function of Z in Ref. [1]; the relevant collisional rate coefficients for the $n=2$ levels may be found in Ref. [33]. The Einstein coefficient A_{ul} scales approximately as $Z^{4.2}$; the collisional rate coefficients as $Z^{-3.2}$, leading to a very sharp dependence: $\epsilon \sim Z^{-7.4}$. The collisional quenching probability for Si He-α, for instance, is only about half that for an identical Al plasma, with a difference of only one atomic number. The scaling of escape probability P_e is considerably weaker. According to Eq. (11), the faster decay rate for higher-atomic-number elements partially compensates the much-lower collisional quenching, but (neglecting the weak scaling of P_e) the escape time can increase with atomic number as fast as $Z^{3.2}$. Stated another way, plasma density must be increased along with atomic number to maintain the ratio of collisional to radiative processes and thereby prevent additional broadening of the line photon emission pulse.

IV. CONCLUDING REMARKS

In plasmas containing mostly K-shell ionization stages, the strongest resonance line (He-α) is usually a significant if not dominant component of the x-ray emission. This is true of plasmas lasting several ns, such as the dense Z pinch, as well as of plasmas produced by ultrashort-pulse lasers which may persist for ps time scales or shorter. Photons emitted in this line as well as other strong resonance lines can be subject to many absorptions and reemissions in optically thick plasmas. In general, this time broadens the line component of the x rays.

This paper has presented detailed numerical calculations supplemented and interpreted by an analytic model which demonstrate that for laboratory plasmas of moderate density and mm or smaller size, the escape time is a few ps or less. These models could also be employed in analyzing astrophysical scale plasmas, where much longer characteristic times are expected. One current goal of experiments employing high-power sub-ps lasers is to produce the shortest possible x-ray pulse. If the entire laser-produced plasma is of solid density, collisional quenching of the line photons assures that the scattering mechanism plays no role in widening the x-ray pulse. However, to date the most efficient x-ray generation has occurred when a preformed plasma created by a laser prepulse is subsequently irradiated by the main high-intensity pulse. The persistence of the heliumlike ground state raises the possibility that a photon-scattering surrounding plasma, even though much cooler than the principal x-ray-generating region, may place a lower limit on the width of the x-ray pulse. Perhaps the use of mostly continuum emission or lines of other ionization stages which may be more subject to collisional quenching would ameliorate this effect. The enhancement of the line escape probability due to the motional Doppler shift may further reduce its importance in some instances. The time-dependent transfer of radiation in strong resonance lines is one of several physical processes which determine the shape and intensity of the x-ray emission from the new class of ultrashort-lived laser-produced plasmas.

ACKNOWLEDGMENTS

The author thanks M. Busquet (CEA Limeil-Valenton, France) for valuable comments. This work was supported by the Office of Innovative Science and Technology of the Strategic Defense Initiative Organization, and the Office of Naval Research.

[1] C. D. Lin, W. R. Johnson, and A. Dalgarno, Phys. Rev. A **15**, 154 (1977).
[2] M. M. Murnane, H. C. Kapteyn, M. D. Rosen, and R. W. Falcone, Science **251**, 531 (1991).
[3] C. H. Nam, W. Tighe, S. Suckewer, J. F. Seely, U. Feldman, and L. A. Woltz, Phys. Rev. Lett. **59**, 2427 (1987).
[4] M. M. Murnane, H. C. Kapteyn, and R. W. Falcone, Phys. Rev. Lett. **62**, 155 (1989).
[5] J. A. Cobble *et al.*, Phys. Rev. A **39**, 454 (1989).
[6] J. C. Kieffer *et al.*, Phys. Rev. Lett. **62**, 760 (1989).
[7] J. A. Cobble, G. T. Schappert, L. A. Jones, A. J. Taylor, G. A. Kyrala, and R. D. Fulton, J. Appl. Phys. **69**, 3369

(1991).
[8] A. Zigler *et al.*, Appl. Phys. Lett. **59**, 534 (1991).
[9] A. Zigler *et al.*, Opt. Lett. **16**, 1261 (1991).
[10] U. Teubner, G. Kuhnle, and F. P. Schafer, Appl. Phys. Lett. **59**, 2672 (1991).
[11] W. M. Wood, C. W. Siders, and M. C. Downer, Phys. Rev. Lett. **67**, 3523 (1991).
[12] M. M. Murnane, H. C. Kapteyn, and R. W. Falcone, Phys. Fluids B **3**, 2409 (1991).
[13] S. E. Harris and J. E. Kmetec, Phys. Rev. Lett. **61**, 62 (1988).
[14] M. D. Rosen, in *Scaling Laws for Femtosecond Laser Plasma Interactions,* edited by E. M. Campbell, SPIE Conf. Proc. No. 1229 (SPIE, Los Angeles, 1990), p. 160.
[15] V. V. Kolchin and S. A. Shlenov, Kvant. Elektron. (Moscow) **18**, 277 (1991) [Sov. J. Quantum Electron. **21**, 247 (1991)].
[16] H. M. Milchberg, I. Lyubomirsky, and C. G. Durfee III, Phys. Rev. Lett. **67**, 2654 (1991).
[17] G. A. Kyrala, R. D. Fulton, E. K. Wahlin, L. A. Jones, G. T. Schappert, J. A. Cobble, and A. J. Taylor, Appl. Phys. Lett. **60**, 2195 (1992).
[18] J. Cooper and P. Zoller, Astrophys. J. **277**, 813 (1984).
[19] S. Chandrasekhar, *Radiative Transfer* (Dover, New York, 1960), pp. 61 and 62.
[20] D. Duston and J. Davis, Phys. Rev. A **23**, 2602 (1981).
[21] T. R. Young and J. P. Boris, J. Phys. Chem. **81**, 2424 (1977).
[22] P. B. Kunasz and D. G. Hummer, Mon. Not. R. Astron. Soc. **166**, 19 (1974).
[23] T. Holstein, Phys. Rev. **72**, 1212 (1947).
[24] J. P. Apruzese, J. Davis, D. Duston, and K. G. Whitney, J. Quant. Spectrosc. Radiat. Transfer **23**, 479 (1980).
[25] J. P. Apruzese, J. Quant. Spectrosc. Radiat. Transfer **34**, 447 (1985).
[26] J. C. Weisheit, J. Quant. Spectrosc. Radiat. Transfer **22**, 585 (1979).
[27] R. C. Mancini, R. F. Joyce, and C. F. Hooper, Jr., J. Phys. B **20**, 2975 (1987).
[28] V. V. Sobelev, Astron. Zh. **34**, 694 (1957) [Sov. Astron. **1**, 678 (1957).
[29] A. I. Shestakov and D. C. Eder, J. Quant. Spectrosc. Radiat. Transfer **42**, 483 (1989).
[30] D. Mihalas, *Stellar Atmospheres,* 2nd ed. (Freeman, San Francisco, 1978), p. 378.
[31] D. E. Osterbrock, Astrophys. J. **135**, 195 (1962).
[32] G. B. Rybicki and D. G. Hummer, Mon. Not. R. Astron. Soc. **144**, 313 (1965).
[33] H. Zhang and D. H. Sampson, Astrophys. J. Suppl. Ser. **63**, 487 (1987).
[34] P. C. Kepple and J. E. Rogerson, Naval Research Laboratory Memorandum Report No. 4216, 1980 (unpublished).
[35] H. R. Grien, M. Blaha, and P. C. Kepple, Phys. Rev. A **19**, 2421 (1979).
[36] G. T. Schappert *et al.*, in *Atomic Processes in Plasmas,* Gaithersburg, MD, 1989, edited by Y. K. Kim and R. C. Elton, AIP Conf. Proc. No. 206 (AIP, New York, 1990), p. 217.
[37] X. Liu and D. Umstadter, Phys. Rev. Lett. **69**, 1935 (1992).